

# Synthesis and Characterization of Poly(alkyl-substituted *p*-phenylene ethynylene)s

W. Y. Huang, W. Gao, T. K. Kwei,\* and Y. Okamoto\*

Polymer Research Institute, Polytechnic University, Brooklyn, New York 11201

Received September 26, 2000; Revised Manuscript Received January 17, 2001

**ABSTRACT:** A series of substituted poly(*p*-phenyleneethynylene)s, PPE, were synthesized by alkyne metathesis. The substituents dibutyl **4a**, dioctyl **4b**, ditetradecyl **4c**, di-2-ethylhexyl **4d**, and di-2-cyclohexylethyl **4e** were placed on the 2,5-positions of the phenyl rings. X-ray diffraction studies indicated that the main chains of each polymer were arranged in regular, layered arrays. Liquid crystalline structures were obtained by polarized optical microscopy in PPE **4b**, **4c**, and **4d**. The temperatures of isotropization of the liquid crystalline structures coincided with the disordering temperatures determined by differential scanning calorimetry. The UV absorption spectra showed a gradual blue shift of the  $\lambda_{\text{max}}$  from **4a** to **4e**, suggesting a decrease in the electronic delocalization along the chain as the size and geometry of the side group changed. The photoluminescence spectra in dilute toluene solutions are consistent with vibronic coupling and emission from localized excited states. The emission spectra of thin films show characteristics typical excimer or aggregate formation in the solid state. Last, an improved method of molecular weight determination by end group analysis was devised.

## Introduction

Electroluminescence devices utilizing  $\pi$ -conjugated polymers as emitting layers have become a subject of great interest since the first report of electroluminescence devices (ELDs) based on poly(phenylenevinylene) (PPV) in 1990.<sup>1</sup> Recently, the acetylene analogues of PPV, based on the phenyl ethynyl unit, the poly-(phenylene ethynylene)s (PPEs) received increasing attention, mainly due to their conjugated rigid-rod-like character and to their optical and electronic applications. These conjugated polymers were used as light-emitting diodes (LEDs),<sup>2,3</sup> plastic lasers,<sup>4</sup> light-emitting electrochemical cells (LECs),<sup>5,6</sup> and polarizers in LC displays.<sup>7</sup> The attractive combination of excellent optical and electronic properties of the conjugated PPEs has motivated our synthesis of new derivatives (Scheme 1) for electroluminescent device applications.

The classical method to synthesize PPEs and related poly(arylene ethynylene)s is the Pd/Cu-catalyzed coupling of dihalogenated (Br, I) arenes or benzenes to diethynylated aromatics in amines as solvents.<sup>8–13</sup> However, as reported in the literature,<sup>14,15</sup> these Pd-catalyzed couplings have several distinct shortcomings, such as the formation of low molecular weight polymers with structure defects and ambiguous end groups. Therefore, an attractive alternative, alkyne metathesis, reported by Bunz et al.<sup>14</sup> was adopted as the method of polymerization in this study.

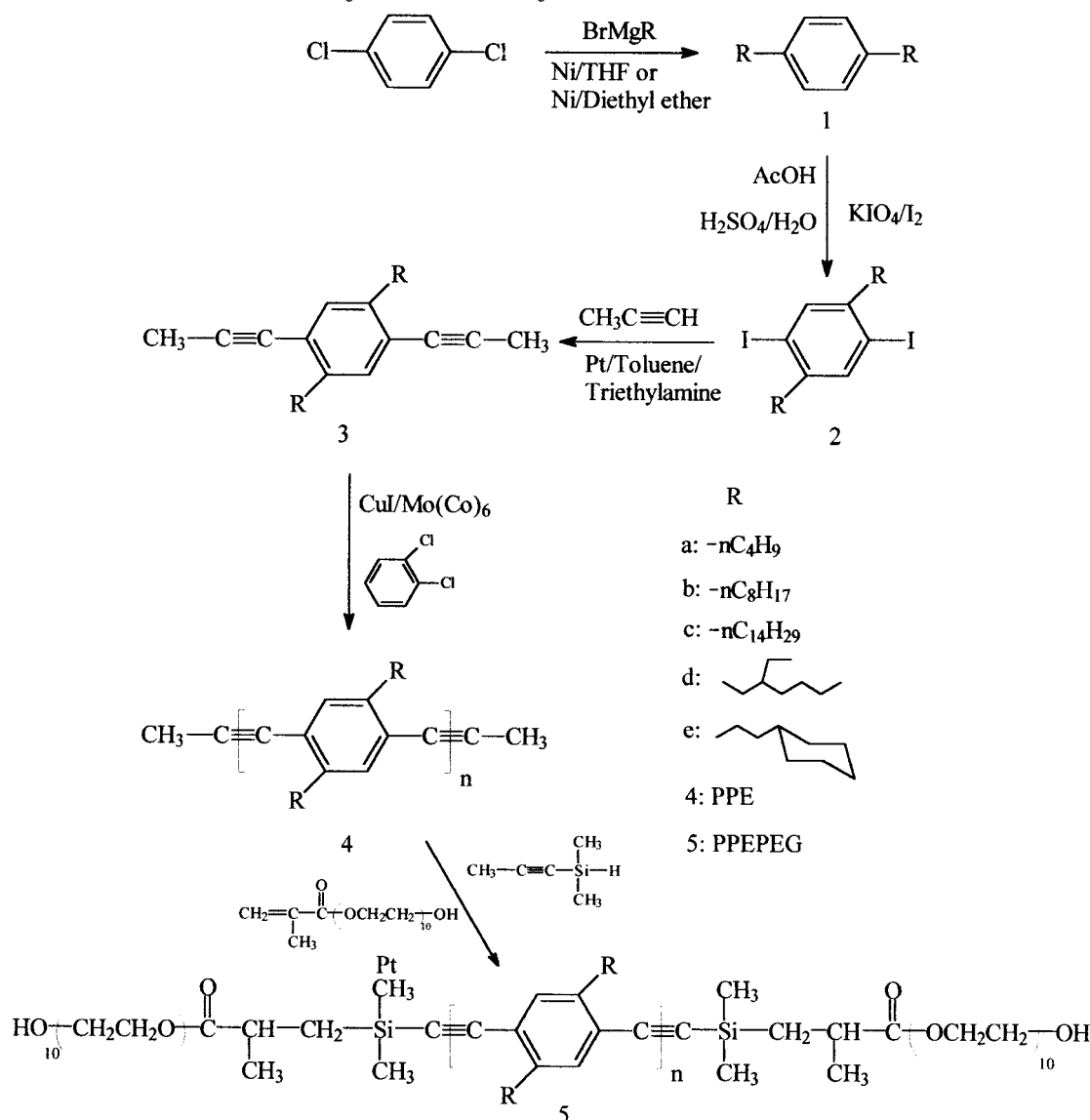
Alkyl substituents improve the solubilities of PPE's in organic solvents, as demonstrated by Bunz<sup>14,15</sup> and West<sup>10</sup> among others,<sup>16–18</sup> thus facilitating the investigations of their properties in the solid and in the solution states. Results of X-ray and microscopy studies were reported by these authors. Building on these information, we have synthesized a series of such polymers with linear and branched side groups (Scheme 1). The purpose of our research is manifold. First, we wish to explore the relation between the structure of the substituent and the affinity of the polymer to display liquid crystalline morphology. Our second goal is to correlate the disordering temperature determined by

calorimetry with the temperature of isotropization of the liquid crystalline morphology as detected by optical microscopy. Third, we tried to determine higher order X-ray reflections, which were expected of layered structures commonly seen in rodlike polymers. Last, the fluorescence of these polymers in solution and in the solid state was also investigated. In the course of our study, we have also devised a more accurate method of molecular weight determination by end group analysis. The method will be briefly described.

## Experimental Section

**Characterization.** <sup>1</sup>H and <sup>13</sup>C NMR spectra were collected on a Bruker ACF 300 spectrometer in chloroform-*d* as solvent and tetramethylsilane (TMS) as the internal standard. The fluorescence spectra were recorded by using Perkin-Elmer LS-50B luminescence spectrophotometer with a xenon lamp as the light source, where a 1 cm quartz cuvette in the right angle geometry at room temperature was used for dilute solution measurement and the solid-state emission was performed in the 30°/60° angle geometry. UV spectra were recorded by Shimadzu UV-2200 spectrophotometer. Thermogravimetric analysis (TGA) was conducted on a TA Instruments 5200 system with a Hi-Res TGA 2950 thermogravimetric analyzer under a heating rate of 20 °C/min and a nitrogen flow rate of 100 cm<sup>3</sup>/min. Differential scanning calorimetry (DSC) was run on a DSC 2920 module in conjunction with the TA Instrument 5200 system. All melting temperature ( $T_m$ ) and glass transition ( $T_g$ ) were obtained using DSC, where the peak maximum and reflection point of the glass transition were taken as  $T_m$  and  $T_g$ , respectively. GPC analysis was conducted with a Waters 510 HPLC system equipped with Waters Styragel HR 5, 4, 3, and 1 (7.8 mm i.d.  $\times$  300 mm) columns in series using polystyrene as the standard and chloroform as the eluent. An optical microscope (Nikon Optiphot) equipped with crossed polarizers and a hot stage (Mettler 82) was employed to observe morphological features and phase transitions of the polymers. X-ray diffraction patterns were obtained from a Philips 3100 X-ray generator with a Philips APD-3720 diffractometer, in which the high-intensity monochromatic Cu K $\alpha$  radiation with an average wavelength 1.5418 Å was generated. Optical quality thin films of polymers were obtained by solvent casting or spin coating from toluene solutions onto quartz substrates. All the films were dried at 60 °C for 24 h

Scheme 1. Synthesis and Polymerization of Monomers 3a–e



in a vacuum before measurement. Film thickness is in the range of several hundred nanometers (spin coatings) to about 25  $\mu\text{m}$  (solvent castings).

**Materials.** All reagents and solvents were purchased from Aldrich Chemical Co., Lancaster, or Fisher. Spectroscopic grade toluene was used for all absorption and emission experiments. *o*-Dichlorobenzene was purchased as dry solvent and used as received. Diethyl ether and tetrahydrofuran (THF) were dried over sodium benzophenone and distilled under argon atmosphere before use. Triethylamine (TEA) was dried over KOH, and toluene was dried over CaH. Both solvents were then distilled under argon atmosphere and deoxygenated by purging with argon for 30 min before use in monomer synthesis. All polymerizations were conducted using standard vacuum-line techniques, and in order to remove butyne produced by the reaction, a slow stream of argon was passed through the reaction vessel during the course of polymerization.

**Monomer Synthesis.** For successful preparation of PPE 4a–e via alkyne metathesis, the corresponding monomers 3a–e have to be prepared in large quantities and good yields (Scheme 1). While 3d was already known and described in the literature,<sup>14,15</sup> the synthetic procedures for the other derivatives of 3 are provided below. Kumada coupling<sup>19</sup> of 1,4-dichlorobenzene with 2.1 equiv of an alkyl Grignard reagent in dry THF at reflux temperature afforded 1,4-dialkylbenzenes 1a–e in good yields, which were iodinated after distillation

or recrystallization without further characterization. Iodination of 1,4-dialkylbenzenes with  $\text{I}_2$  and  $\text{KIO}_4$  in a solvent mixture of acetic acid, sulfuric acid, and chloroform gave diiodides 2a–e in fair to good yields. Propynylations of 2a–e were carried out using Heck reaction<sup>8</sup> with 2.2 equiv of propyne in a dry solvent mixture of toluene and triethylamine furnished monomers 3a–e in good to excellent yields. The detailed procedure for each precursor is given separately below.

**General Procedure for Preparation of 1a–e.** All 1,4-dialkylbenzenes were prepared by the reaction of 1,4-dichlorobenzene with Grignard reagents according to a previously published procedure.<sup>14</sup> To a solution of 2.2 equiv of alkylmagnesium bromide in anhydrous ethyl ether or THF was slowly added 1 equiv of 1,4-dichlorobenzene and a catalytic amount of 1,3-bis(diphenylphosphino)propane nickel chloride (dppp-NiCl<sub>2</sub>). The reaction mixture was stirred at reflux temperature for 24 h. The mixture was poured onto icily diluted HCl aqueous solution and extracted with chloroform (3  $\times$  100 mL). The combined organic layers were washed with H<sub>2</sub>O (3  $\times$  100 mL) and dried over MgSO<sub>4</sub>. Then the solvent was removed under reduced pressure, and the resultant was purified by distillation or recrystallization. The above procedure was used in the synthesis of 1a–e.

**1,4-Dibutylbenzene (1a).** 1,4-Dichlorobenzene (20.0 g, 136 mmol), dpppNiCl<sub>2</sub> (0.175 g, 0.320 mmol), and butylmagnesium bromide [Mg (7.34 g, 299 mmol), 1-bromobutane (41.0 g, 299 mmol) in 300 mL of anhydrous diethyl ether] gives 1a as a

colorless oil (17.6 g, 68%); bp 104 °C (0.05 Torr). <sup>1</sup>H NMR (CDCl<sub>3</sub>): δ 7.21 (s, 4H), 2.70 (t, 4H), 1.72 (m, 4H), 1.48 (m, 4H), 1.04 (t, 6H).

**1,4-Diethylbenzene (1b).** 1,4-Dichlorobenzene (20.0 g, 136 mmol), dpppNiCl<sub>2</sub> (0.175 g, 0.320 mmol), and octylmagnesium bromide [Mg (7.34 g, 299 mmol), 1-bromooctane (57.7 g, 299 mmol) in 300 mL of anhydrous THF] gives **1b** as a colorless oil (26.7 g, 65%); bp 121 °C (0.05 Torr). <sup>1</sup>H NMR (CDCl<sub>3</sub>): δ 7.05 (s, 4H), 2.52 (t, 4H), 1.62 (m, 4H), 1.31 (m, 20H), 0.90 (t, 6H).

**1,4-Ditetradecylbenzene (1c).** 1,4-Dichlorobenzene (20.0 g, 136 mmol), dpppNiCl<sub>2</sub> (0.175 g, 0.320 mmol), and tetradecylmagnesium bromide [Mg (7.34 g, 299 mmol), 1-bromooctane (82.8 g, 299 mmol) in 500 mL of anhydrous THF] gives **1c** as a white solid recrystallized from ethanol (58.7 g, 82%); mp 43 °C. <sup>1</sup>H NMR (CDCl<sub>3</sub>): δ 7.03 (s, 4H), 2.56 (t, 4H), 1.59 (m, 4H), 1.29 (m, 44H), 0.90 (t, 6H).

**1,4-Bis(2-ethyl)hexylbenzene (1d).** 1,4-Dichlorobenzene (10.0 g, 68 mmol), dpppNiCl<sub>2</sub> (0.087 g, 0.160 mmol), and Grignard solution [Mg (3.67 g, 150 mmol), 1-bromo-2-ethylhexane (28.9 g, 150 mmol) in 150 mL of anhydrous THF] gives **1d** as a colorless oil (9.9 g, 48%); bp 146 °C (0.05 Torr). <sup>1</sup>H NMR (CDCl<sub>3</sub>): δ 7.05 (s, 4H), 2.51 (t, 4H), 1.55 (m, 2H), 1.30 (m, 16H), 0.90 (t, 12H).

**1,4-Bis(2-cyclohexyl)ethylbenzene (1e).** 1,4-Dichlorobenzene (20.0 g, 136 mmol), dpppNiCl<sub>2</sub> (0.175 g, 0.320 mmol), and Grignard solution [Mg (7.34 g, 299 mmol), 1-bromo-2-cyclohexylethane (57.7 g, 299 mmol) in 300 mL of anhydrous THF] gives **1e** as a needle crystal recrystallized from ethyl acetate (32.4 g, 79%); mp 46 °C. <sup>1</sup>H NMR (CDCl<sub>3</sub>): δ 7.08 (s, 4H), 2.59 (t, 4H), 1.75 (m, 10H), 1.50 (m, 4H), 1.22 (m, 8H), 0.94 (m, 4H).

**Preparation of 1,4-Dialkyl-2,5-diiodobenzenes (2a–e).** The procedure for the preparation of 1,4-dialkyl-2,5-diiodobenzenes was adapted from ref 14.

**1,4-Dibutyl-2,5-diiodobenzene (2a).** To a solution of **1a** (23.0 g, 121 mmol), 200 mL of acetic acid, 15 mL of H<sub>2</sub>O, and 7 mL of concentrated H<sub>2</sub>SO<sub>4</sub> was added KIO<sub>4</sub> (33.4 g, 145 mmol) and I<sub>2</sub> (36.9 g, 145 mmol). The reaction mixture was stirred at 80 °C for 24 h. The mixture was poured into a Na<sub>2</sub>SO<sub>3</sub> aqueous solution (20%) and extracted with hexane (3 × 100 mL). The combined organic layers were washed with H<sub>2</sub>O (3 × 100 mL) and dried over MgSO<sub>4</sub>. Then the solvent was removed under reduced pressure, and the resultant was purified first by chromatography using silica gel as packing material and hexane as eluent and then by recrystallization twice from ethanol. The pure product was obtained as a white solid (21.0 g, 40%); mp 50 °C. <sup>1</sup>H NMR (CDCl<sub>3</sub>): δ 7.41 (s, 2H), 2.40 (t, 4H), 1.35 (m, 4H), 1.21 (m, 4H), 0.78 (t, 6H).

**1,4-Diethyl-2,5-diiodobenzene (2b).** To a solution of **1b** (30.1 g, 99.7 mmol), 200 mL of acetic acid, 16 mL of H<sub>2</sub>O, and 7 mL of concentrated H<sub>2</sub>SO<sub>4</sub> was added KIO<sub>4</sub> (27.6 g, 120 mmol) and I<sub>2</sub> (30.6 g, 120 mL). The reaction mixture was stirred at 90 °C for 24 h. The mixture was poured into a Na<sub>2</sub>SO<sub>3</sub> aqueous solution (20%) and stirred at room temperature for 30 min. After filtration a slightly brown solid was collected. The pure product (45.6 g, 83%) was obtained by recrystallization twice from ethanol; mp 58 °C. <sup>1</sup>H NMR (CDCl<sub>3</sub>): δ 7.62 (s, 2H), 2.60 (t, 4H), 1.58 (m, 4H), 1.35 (m, 20H), 0.90 (t, 6H).

**1,4-Ditetradecyl-2,5-diiodobenzene (2c).** To a solution of **1c** (47.0 g, 100 mmol), 300 mL of acetic acid, 100 mL of chloroform, 24 mL of H<sub>2</sub>O, and 10 mL of concentrated H<sub>2</sub>SO<sub>4</sub> was added KIO<sub>4</sub> (27.6 g, 120 mmol) and I<sub>2</sub> (30.6 g, 120 mL). The reaction mixture was stirred at 100 °C for 48 h. The mixture was poured into a Na<sub>2</sub>SO<sub>3</sub> aqueous solution (20%) and stirred at room temperature for 30 min. The precipitate was then filtered and recrystallized twice from solvent mixture of ethanol/chloroform. The pure product (53.2 g, 71%) was obtained as a white solid; mp 63 °C. <sup>1</sup>H NMR (CDCl<sub>3</sub>): δ 7.54 (s, 2H), 2.55 (t, 4H), 1.51 (m, 8H), 1.23 (m, 40H), 0.84 (t, 6H).

**1,4-Bis(2-ethyl)hexyl-2,5-diiodobenzene (2d).** To a solution of **1d** (10.8 g, 36 mmol), 100 mL of acetic acid, 8 mL of H<sub>2</sub>O, and 3.5 mL of concentrated H<sub>2</sub>SO<sub>4</sub> was added KIO<sub>4</sub> (9.89 g, 43 mmol) and I<sub>2</sub> (10.9 g, 43 mL). The reaction mixture was stirred at 90 °C for 24 h. The mixture was poured into a Na<sub>2</sub>SO<sub>3</sub> aqueous solution (20%) and extracted with hexane (3 × 100 mL). The combined organic layers were washed with H<sub>2</sub>O (3 × 100 mL) and dried over MgSO<sub>4</sub>. Then the solvent was removed under reduced pressure, and the resultant was purified by distillation, column chromatography, or recrystallization. The above procedure was used in the synthesis of **3a–e**.

SO<sub>3</sub> aqueous solution (20%) and extracted with hexane (3 × 100 mL). The combined organic layers were washed with H<sub>2</sub>O (3 × 100 mL). Then the solvent was removed under reduced pressure. After distillation, a pale yellow liquid (7.38 g, 37%) was obtained. <sup>1</sup>H NMR (CDCl<sub>3</sub>): δ 7.49 (s, 2H), 2.48 (t, 4H), 1.60 (m, 2H), 1.22 (m, 16H), 0.82 (t, 12H).

**1,4-Bis(2-cyclohexyl)ethyl-2,5-diiodobenzene (2e).** A mixture of compound **1e** (3.60 g, 12 mmol), KIO<sub>4</sub> (3.30 g, 14 mmol), I<sub>2</sub> (3.70 g, 14 mL), 50 mL of acetic acid, 4 mL of H<sub>2</sub>O, and 1.8 mL of concentrated H<sub>2</sub>SO<sub>4</sub> was stirred at 90 °C for 24 h. The mixture was poured into a Na<sub>2</sub>SO<sub>3</sub> aqueous solution (20%) and stirred at room temperature for 30 min. After filtration a slightly brown solid was collected. The white crystal (5.40 g, 82%) was obtained by recrystallization twice from a ethanol/chloroform mixed solvent; mp 87 °C. <sup>1</sup>H NMR (CDCl<sub>3</sub>): δ 7.51 (s, 2H), 2.52 (t, 4H), 1.67 (m, 10H), 1.34 (m, 4H), 1.20 (m, 8H), 0.89 (t, 4H).

**General Procedure for the Preparation of the Monomers (3a–e).** Propynylations of **2a–e** were carried out using Heck reaction<sup>8</sup> with 2.2 equiv of propyne in dry solvent mixture of toluene and triethylamine furnished monomers **3a–e** in good to excellent yields. The detailed procedure for each monomer is given separately below.

One equiv mol of 1,4-diiodo-2,5-dialkylbenzene (**2**), 0.05 equiv mol of Pd(PPh<sub>3</sub>)<sub>2</sub>Cl<sub>2</sub>, and 0.1 equiv mol of CuI were placed in a flame-dried flask. A proper amount of toluene/triethylamine (5/1) was injected into the reaction vessel via syringe through a septum. Before the reaction was taken place, the solution was purged with a slow stream of argon for 10 min, and then 2.2 equiv mol of propyne was introduced into the solution. The reaction mixture was stirred for several more hours at room temperature. The resultant mixture was then passed through a short column packed with silica gel. Evaporation of solvent yields a crude product, which is purified by distillation, column chromatography, or recrystallization. The above procedure was used in the synthesis of **3a–e**.

**2,5-Dibutyl-1,4-dipropynylbenzene (3a).** **2a** (20.2 g, 45.6 mmol), Pd(PPh<sub>3</sub>)<sub>2</sub>Cl<sub>2</sub> (1.60 g, 2.28 mmol), CuI (0.868 g, 4.56 mmol), propyne (4.01 g, 100 mmol), triethylamine (65 mL), and toluene (350 mL) give **3a** as a slightly yellow liquid purified from silica gel column chromatography (10.4 g, 86%). <sup>1</sup>H NMR (CDCl<sub>3</sub>): δ 7.22 (s, 2H), 2.22 (t, 4H), 2.14 (s, 6H), 1.63 (m, 4H), 1.40 (m, 4H), 0.99 (t, 6H).

**2,5-Diethyl-1,4-dipropynylbenzene (3b).** **2b** (11.1 g, 20.0 mmol), Pd(PPh<sub>3</sub>)<sub>2</sub>Cl<sub>2</sub> (0.70 g, 1.00 mmol), CuI (0.380 g, 2.00 mmol), propyne (1.76 g, 40.0 mmol), triethylamine (40 mL), and toluene (250 mL) give **3b** as a yellow solid recrystallized from ethanol twice (6.11 g, 80%); mp 53 °C. <sup>1</sup>H NMR (CDCl<sub>3</sub>): δ 7.12 (s, 2H), 2.69 (t, 4H), 2.09 (s, 6H), 1.60 (m, 4H), 1.34 (m, 20H), 0.95 (t, 6H). <sup>13</sup>C NMR (CDCl<sub>3</sub>): δ 144.3, 134.2, 124.8, 92.2, 81.4, 36.5, 34.5, 33.2, 31.9, 31.8, 25.4, 17.0, 7.2.

**2,5-Ditetradecyl-1,4-dipropynylbenzene (3c).** **2c** (31.1 g, 40.2 mmol), Pd(PPh<sub>3</sub>)<sub>2</sub>Cl<sub>2</sub> (1.41 g, 2.01 mmol), CuI (0.770 g, 4.02 mmol), propyne (3.53 g, 88.4 mmol), triethylamine (70 mL), and toluene (400 mL) give **3c** as a slightly yellow solid recrystallized from ethanol twice (18.7 g, 85%); mp 60 °C. <sup>1</sup>H NMR (CDCl<sub>3</sub>): δ 7.18 (s, 2H), 2.67 (t, 4H), 2.10 (s, 6H), 1.63 (m, 4H), 1.32 (m, 44H), 0.93 (t, 6H).

**2,5-Bis(ethyl)hexyl-1,4-dipropynylbenzene (3d).** **2d** (14.6 g, 26.4 mmol), Pd(PPh<sub>3</sub>)<sub>2</sub>Cl<sub>2</sub> (0.920 g, 1.30 mmol), CuI (0.501 g, 2.64 mmol), propyne (2.30 g, 58.1 mmol), triethylamine (35 mL), and toluene (200 mL) give **3d** as a yellow solid recrystallized from ethanol twice (5.26 g, 53%); mp 65 °C. <sup>1</sup>H NMR (CDCl<sub>3</sub>): δ 7.06 (s, 2H), 2.52 (m, 4H), 2.01 (s, 6H), 1.58 (m, 2H), 1.20 (m, 16H), 0.81 (t, 12H).

**2,5-Bis(cyclohexyl)ethyl-1,4-dipropynylbenzene (3e).** **2e** (5.25 g, 9.50 mmol), Pd(PPh<sub>3</sub>)<sub>2</sub>Cl<sub>2</sub> (0.330 g, 0.470 mmol), CuI (0.181 g, 0.950 mmol), propyne (0.830 g, 20.9 mmol), triethylamine (15 mL), and toluene (80 mL) give **3e** as a yellow crystal recrystallized from ethanol twice (2.65 g, 73%); mp 85 °C. <sup>1</sup>H NMR (CDCl<sub>3</sub>): δ 6.98 (s, 2H), 2.45 (t, 4H), 1.90 (s, 6H), 1.63 (m, 4H), 1.55 (m, 10H), 1.29 (m, 4H), 1.06 (m, 8H), 0.77 (m, 4H).

**General Procedure for the Polymerizations.** In a typical reaction, **3** (1.00 g) and the catalyst system consisting



Table 1. General Properties of PPE 4a–e

polymer	4a	4b	4b'	4c	4d	4e
R	<i>n</i> -butyl	<i>n</i> -octyl	<i>n</i> -octyl	<i>n</i> -tetradecyl	2-ethylhexyl	2-cyclohexylethyl
reaction time (h)	24	24	48	24	24	24
amt of monomer <b>3</b> , g (mmol)	2.00 (7.50)	4.50 (11.9)	6.97 (18.4)	3.00 (5.46)	1.06 (2.81)	2.16 (5.71)
yield PPE4, g (%)	1.44 (95)	3.85 (<99)	5.91 (99)	2.62 (97)	0.84 (97)	1.76 (95)
$P_n/M_n$ ( $^1\text{H}$ NMR) <sup>a</sup>	<i>c</i>	26/8454	45/14610	21/10362	25/8100	<i>d</i>
$P_n/M_n$ ( $^1\text{H}$ NMR) <sup>b</sup>	98/20806	22/7128	43/13932	19.9378	24/7806	51/16554
$P_n/M_n$ (GPC)	201/42642	42/13700	84/27300	37/18234	48/15582	<i>d</i>
$M_w/M_n$ (GPC)	2.84	2.94	1.81	1.44	1.92	<i>d</i>

<sup>a</sup>  $P_n$ 's are calculated from the end group analysis of the methyl groups of PPE 4a–e. <sup>b</sup>  $P_n$ 's are calculated from the end group analysis of the ethylene groups of triblock copolymer 5a–e. <sup>c</sup> The end groups of methyl are too small to be detectable for PPE 4a. <sup>d</sup> Because of poor solubility of PPE 4e, these values could not be obtained.

of Mo(CO)<sub>6</sub> (5 mol %)/*p*-chlorophenol are dissolved in 50 mL of *o*-dichlorobenzene. The solution was stirred at 150 °C overnight, and a slow stream of argon was passed through the reaction vessel during the course of polymerization for removing the butyne, produced by the reaction. For work-up, the resultant polymer solution was poured into a stirring methanol, and the yellow polymer was precipitated in situ. The precipitated polymer **4** was collected by filtration and washed with 10% HCl and H<sub>2</sub>O and then vacuum-dried until no solvent was detected in TGA experiment. For yields and amounts, see Table 1.

**Polymer 4a.** Soluble in common organic solvents.  $^1\text{H}$  NMR (CDCl<sub>3</sub>):  $\delta$  7.32 (s, 2H), 2.81 (bs, 4H), 2.02 (s, end group), 1.64 (bs, 4H), 1.36 (bs, 4H), 0.89 (t, 6H).  $^{13}\text{C}$  NMR (CDCl<sub>3</sub>):  $\delta$  142.3, 132.7, 123.2, 93.5, 34.3, 33.1, 23.1, 14.2.

**Polymer 4b.** Soluble in common organic solvents.  $^1\text{H}$  NMR (CDCl<sub>3</sub>):  $\delta$  7.42 (s, 2H), 2.88 (bs, 4H), 2.12 (s, end group), 1.74 (bs, 4H), 1.36 (bs, 20H), 0.89 (bs, 6H).  $^{13}\text{C}$  NMR (CDCl<sub>3</sub>):  $\delta$  141.3, 132.1, 122.5, 92.4, 34.2, 31.8, 30.8, 30.2, 29.7, 22.5, 14.2.

**Polymer 4c.** Partial soluble in toluene. Soluble in chloroform.  $^1\text{H}$  NMR (CDCl<sub>3</sub>):  $\delta$  7.32 (s, 2H), 2.78 (bs, 4H), 2.04 (s, end group), 1.68 (bs, 4H), 1.24 (bs, 44H), 0.82 (bs, 6H).  $^{13}\text{C}$  NMR (CDCl<sub>3</sub>):  $\delta$  142.5, 133.0, 123.5, 93.4, 34.5, 32.4, 31.2, 30.5, 30.2, 30.0, 29.6, 23.2, 14.5.

**Polymer 4d.** Soluble in common organic solvents.  $^1\text{H}$  NMR (CDCl<sub>3</sub>):  $\delta$  7.27 (s, 2H), 2.73 (bs, 4H), 2.02 (s, end group), 1.72 (bs, 4H), 1.28 (bs, 16H), 0.85 (bs, 12H).  $^{13}\text{C}$  NMR (CDCl<sub>3</sub>):  $\delta$  143.7, 136.2, 125.9, 96.4, 43.1, 41.2, 36.2, 31.8, 28.5, 25.9, 17.0, 13.6.

**Polymer 4e.** Partial soluble in chloroform.  $^1\text{H}$  NMR (CDCl<sub>3</sub>):  $\delta$  7.33 (s, 2H), 2.78 (bs, 4H), 2.10 (s, end group), 1.80 (bs, 4H), 1.61 (bs, 10H), 1.20 (bs, 8H), 0.91 (bs, 4H).

**PPEs with the End Group of Si–H.** The solution of 1 equiv mol of PPEs (**4**), 4 equiv mol of 1-propynyldimethylsilane, and the catalyst [Mo(CO)<sub>6</sub> (5 mol %)/*p*-chlorophenol] in a proper amount of toluene was stirred at 80 °C for overnight. The solution was poured into methanol, and the precipitated yellow solid was collected by filtration. The filtrate was dried under vacuum for 24 h. The yield was obtained quantitatively.

General Procedure for the Preparation of the Triblock Copolymers (5a–e). One equiv mol of Si–H end-capped PPE, 2 equiv mol of poly(ethylene glycol)<sub>10</sub> methacrylate, and 0.5% equiv mol of HPTCl<sub>6</sub> were dissolved in toluene. The solution was stirred at reflux under argon atmosphere for overnight. For work-up, the solution was then poured into methanol/H<sub>2</sub>O (50/50), and the polymer suspended solution was stirred for one more hour for removing unreacted poly(ethylene glycol)<sub>10</sub> methacrylate from the resultant copolymer **5**. Copolymer **5** was collected by filtration and vacuum-dried until no solvent was detected in TGA experiment. The NMR spectrum is shown in Figure 2, and molecular weight analysis was discussed below.

## Results and Discussion

**Molecular Weight.** Since the NMR spectra (Figure 1) are in full accord with the expected chemical structures and show no signs of structural inequalities and defects, we sought to use end group analysis to determine the molecular weights of the polymers. In the case

of PPE **4b**, which is quantitatively end-capped with methyl groups, the number-average degree of polymerization ( $P_n$ ) can be determined by comparing the integrated intensities of the methyl end groups (six hydrogens) at 2.1 ppm and the methylene groups (four hydrogens) of the  $\alpha$ -position of *n*-octyl group at 2.7 ppm. This gave a number-average molecular weight,  $M_n$ , of 8454 g/mol and a  $P_n$  of 26. However, this approach is applicable only for low molecular weight polymers. To obtain more accurate  $M_n$  values for higher molecular weight polymers, we need to design an end group that contains a larger number of distinguishable protons. To this end we synthesized an ABA triblock copolymer (5a–e, shown in Scheme 1), which consisted of middle block (B) of PPE and two end-blocks of PEG with 10 repeating units. The  $^1\text{H}$  NMR of **5b** is shown in Figure 2. Again, a similar procedure was applied to calculate the number-average molecular weight ( $M_n$ ) by comparing the integrated intensity of the methylene groups of PEG at 3.6 ppm with the signal of the  $\alpha$ -position methylene groups of PPE at 2.7 ppm. This resulted for **5b** in a number-average molecular weight,  $M_n$ , of 7128 g/mol and a  $P_n$  of 22. The agreement between the two calculations validates the end group analysis method. The other polymers, **4a**, **4c–e**, **5a**, and **5c–e**, show similar NMR spectra. The calculated  $M_n$ 's using the both methods of measurements are shown in Table 1.

The polydispersity indices ( $M_w/M_n$ ) of the polymers were estimated using GPC measurements, relative to polystyrene standards. Since the GPC method using polystyrene calibration is known to lead to significant errors in the determination of the absolute molecular weight in the case of rigid-rod polymers,<sup>14</sup> the molecular weights of PPEs obtained by GPC measurements are expected to deviate from those obtained by  $^1\text{H}$  NMR end group analysis. Indeed, as demonstrated in Table 1, the molecular weights measured by GPC show a consistent and systematic overestimation by a factor about 2 over the molecular weights obtained by  $^1\text{H}$  NMR end group analysis.

**Solid-State Structure.** The supramolecular structures of the polymers were investigated by X-ray diffraction with powder or film samples. In Figure 3, the X-ray scattering profiles of **4a–e** are shown, and the corresponding  $d$  spacings are calculated and tabulated in Table 2. For each sample, there are only broad reflections in the wide-angle region ( $2\theta \sim 20$ – $24^\circ$ ), which indicates a low degree of structural order. The  $d$  spacings of 3.8 and 4.2 Å were assigned<sup>10,15</sup> as the distances of two aromatic ring planes between the rigid rods. In the two polymers, **4d** and **4e**, with bulky side groups, the  $d$  spacing was increased to about 5 Å.

In the  $2\theta < 15^\circ$  region, there are two to three reflections for each polymer. The largest spacing rep-

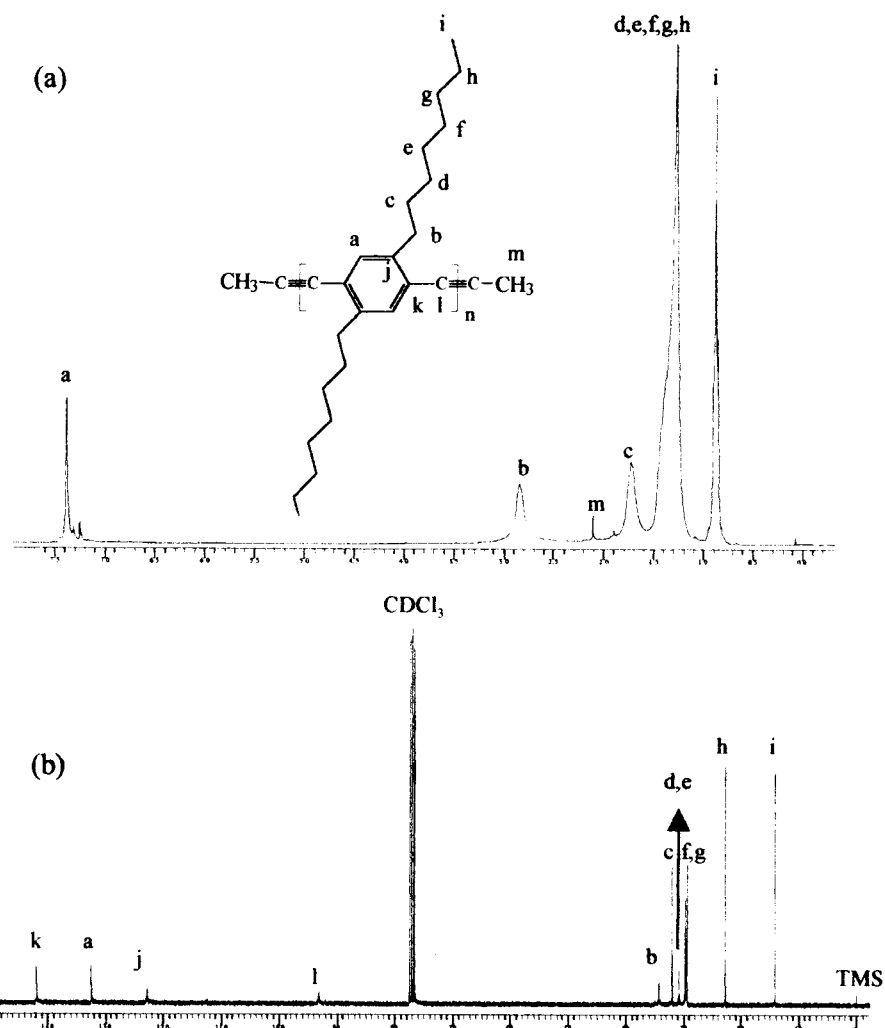


**Figure 1.** (a)  $^1\text{H}$  NMR and (b)  $^{13}\text{C}$  NMR spectra of **4b** in  $\text{CDCl}_3$ .

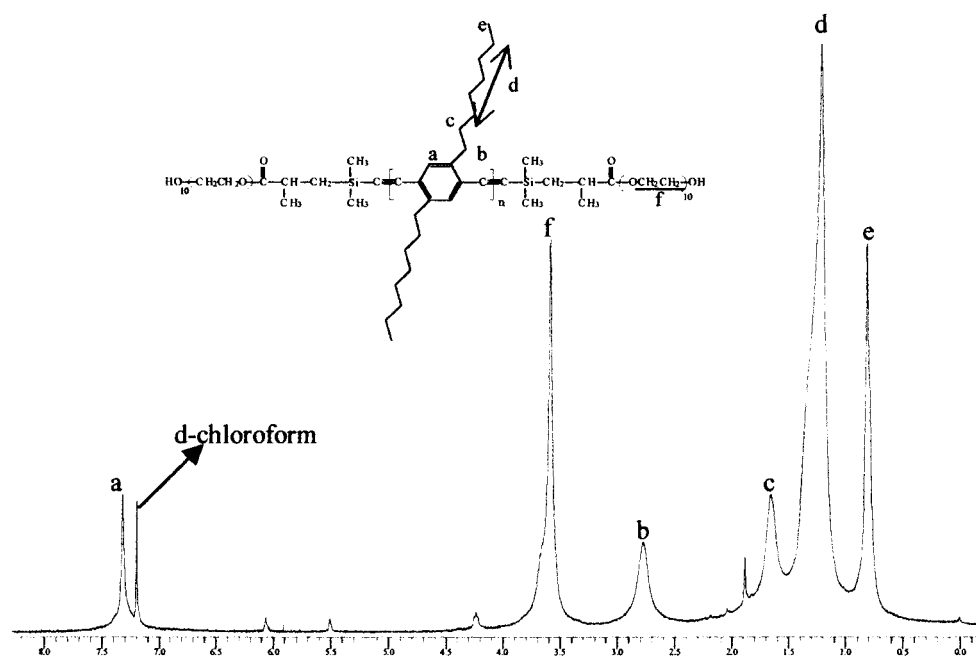


**Figure 2.**  $^1\text{H}$  NMR spectrum of **5b** in  $\text{CDCl}_3$ .

resents the intermolecular distance between two rodlike chains. The smaller spacings are higher-order reflections that correspond to  $1/2$  (second order) and  $1/3$  (third order) or  $1/5$  (fifth order) the value of the first-order

reflection. These results are typical of chains arranged in regular, layered arrays. Since the second-order reflection is usually stronger than the third-order one, the data for **4b** and **4c** seem to violate the rule, but

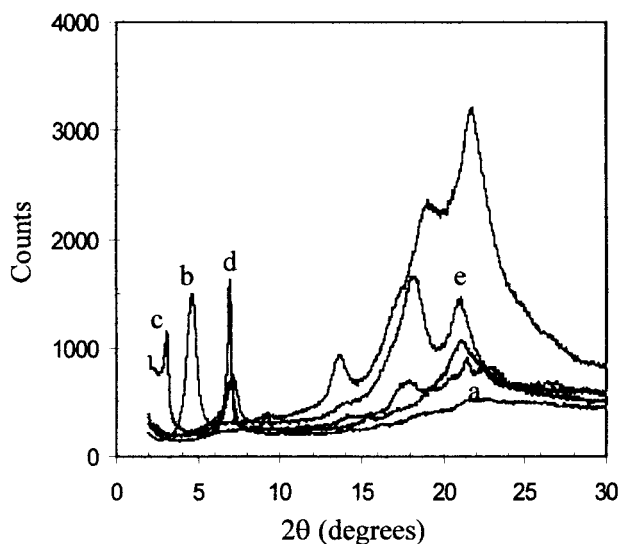


**Figure 3.** WAXS profiles of the as-made PPEs: (a) **4a**, (b) **4b**, (c) **4c**, (d) **4d**, and (e) **4e**.

**Table 2.** WAXS Diffractions (Å) of the As-Made PPEs

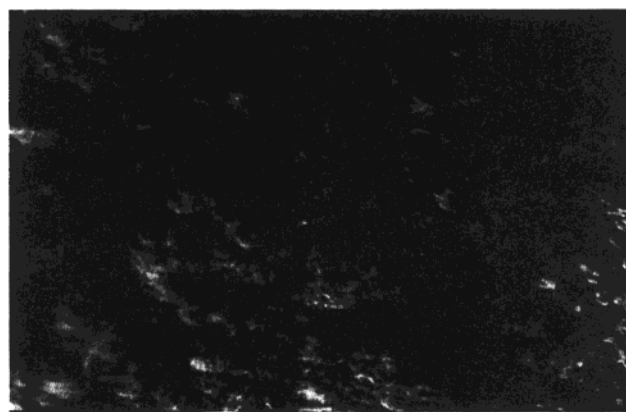
PPE 4a–e	low-angle region			wide-angle region	
<b>4a<sup>a</sup></b>	12.4 (1)	6.2 (2)		4.1	3.8
<b>4b<sup>b</sup></b>	20.5 (1)	10.1 (2)	6.7 (3)	4.2	3.8
<b>4c<sup>a</sup></b>	29.0 (1)	9.6 (3)	5.7 (5)	4.3	3.9
<b>4d<sup>a</sup></b>	12.9 (1)	6.3 (2)		4.3/4.2/4.0	5.0
<b>4e<sup>b</sup></b>	12.3 (1)	6.4 (2)		4.2	4.9

<sup>a</sup> Film. <sup>b</sup> Powder.

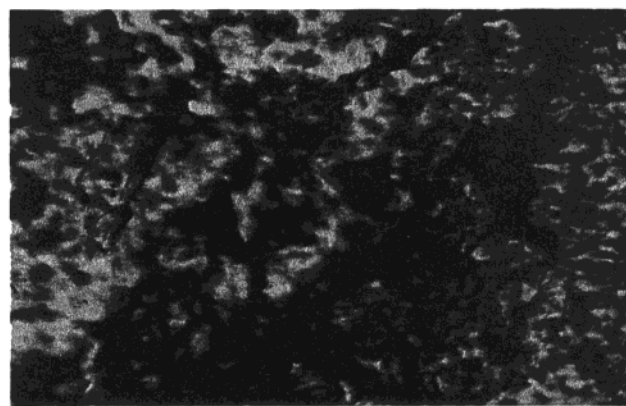
exceptions have been reported in a study of alkyl-substituted hydroxypropylcellulose.<sup>34,35</sup>

From the intermolecular distances, there seems to be no interdigitation of the side chains in **4a** and **4b** if the structure proposed by West<sup>10</sup> is used in the calculation. The spacing of 29.1 Å for C14 disubstituted polymer is consistent with interdigitation of the side chains; alternatively, Wegner et al.<sup>33</sup> have proposed a bilayer model for some alkyl-substituted rigid polymers in which the main chains are aligned in a zigzag pattern and the side chains are not interdigitated but tilted at an angle to the main chain. Our limited X-ray data cannot distinguish the two models. The intermolecular distance of 12.7 Å for the **4d** requires slight interdigitation of the 2-ethylhexyl side group. The same conclusion was reached by Bunz.<sup>15</sup> In the case of polymer **4e**, there seems to be little or no overlap of the cyclohexyl groups from dimensional considerations.

Mesophase behavior is common in hairy rod polymers, such as poly(phenylenevinylene)s (PPVs),<sup>2,20</sup> polythiophenes,<sup>21–23</sup> and some polyphenylenes.<sup>24</sup> The layered structures indicated by X-ray diffraction suggests strongly the presence of liquid crystalline structures. However, such structures were often not detected by optical microscopy due to structural defects and low degree of polymerization, resulting in small axial ratios.<sup>15,25–29</sup> These shortcomings are alleviated to a large extent by the synthetic procedure used here. The photomicrographs taken by Bunz et al.<sup>15</sup> further encouraged us to examine these polymers by polarized optical microscopy (POM) which revealed liquid crystalline structures in the solid and the solution states of **4b**, **4c**, and **4d** (Figure 4). The details of POM studies will be described in a separate publication. In the context of this paper, the microscopy observations are used here only for the



(a)



(b)

**Figure 4.** POM photographs of **4b**: (a) solid film, (b) 20 wt % in 1,2-dichlorobenzene.

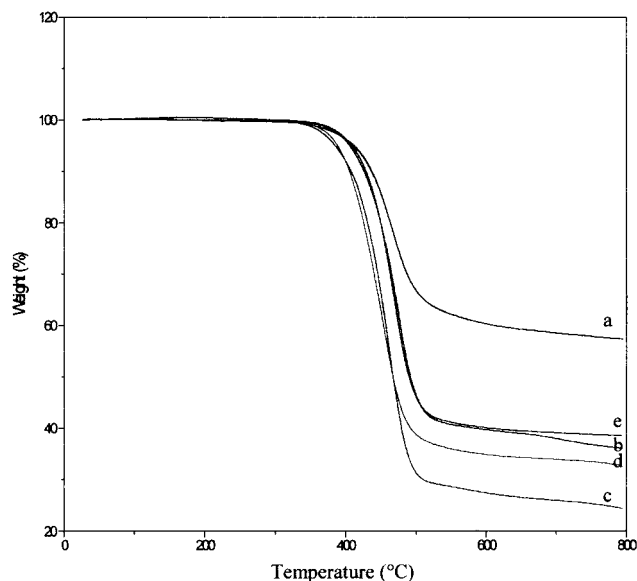


**Figure 5.** TGA thermogram of PPE **4a–e**: (a) **4a**, (b) **4b**, (c) **4c**, (d) **4d**, and (e) **4e**.

purpose of identifying the isotropization temperatures for comparison with the disordering temperatures seen in DSC scans.

**Thermal Properties.** The thermal properties of the polymers were investigated using thermogravimetric analysis (TGA) and differential scanning calorimetry (DSC). In Figure 5 the TGA thermograms for PPE **4a–e** are shown, which indicate two decomposition processes

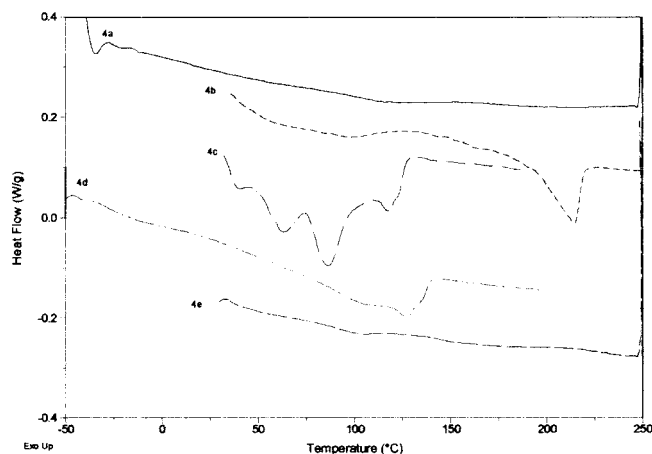


**Figure 6.** DSC thermograms of PPEs: (a) **4a**, (b) **4b**, (c) **4c**, (d) **4d**, and (e) **4e**.

for each of the five polymers. The first process, starting at about 340 °C with weight losses of 43, 63, 76, 61, and 68% for PPE **4a–e**, respectively, was attributed to the degradation of the alkyl side chains. The second process, starting at about 550 °C with char residues of 57, 37, 24, 39, and 32% at 800 °C for PPE **4a–e**, respectively, was attributed to the degradation of the main chain. The initial thermal degradation temperature of about 340 °C was well above the highest temperature (250 °C) used in DSC experiments; furthermore, the samples were solvent-free within the TGA limits of detection. This guarantees that no artifact will be seen in the DSC and microscopy studies, which are shown below.

In the DSC scan of PPE **4a** (Figure 6a), only one endothermic transition was seen at 101 °C, which was attributable to the disordering of the supramolecular structure. For polymer **4b**, the first heating scan showed a broad endothermic event which began as an increase in specific heat followed by a shallow first-order transition spanning 60 to 120 °C. The origin of this transition is an unsettled issue in the literature. Wegner et al.<sup>33</sup> observed a transition at 71 °C in *n*-octyl-disubstituted rigid aromatic polyester which was attributed to side chain motion. On the other hand, thermal transitions were not found in the 45–80 °C region in *n*-octyl-substituted polythiophene (rigid), hydroxylpropylcellulose (semiflexible), and polymethacrylate or polyacrylate (flexible). We propose that the broad endotherm seen in the thermogram of **4b** (Figure 6b) is a mesophase transition induced by side chain motion. We plan to carry out X-ray measurements at different temperatures in hopes of gaining a better understanding of the underlying process. At higher temperatures, a strong endotherm at 215 °C coincided with the temperature of transformation of the mesophase to the isotropic melt as seen by POM.

When the length of the side chain was increased from C8 to C14, the thermogram of **4c** (Figure 6c) showed four distinct transitions. The 39 and 63 °C transitions can be assigned to side chain melting because it is well-known long alkyl groups (>C12) in many rigid or flexible polymer intercalate and develop crystalline structures same as those of paraffinic hydrocarbons. As already mentioned, the interdigitation of C14 side chains is supported by X-ray data. The double melting is due to dual crystalline modifications.<sup>32,34,35</sup> It should be mentioned here that the *d* spacings of the side chain crystals have been determined by many researchers<sup>34,36</sup>

**Table 3.** Thermal Transitions of PPEs

PPE <b>4a–e</b>	$T_g$ , °C	$T_{sc}^a$ , °C	$T_{lc}^b$ , °C	$T_i$ , °C
<b>4a</b>				101
<b>4b</b>		45	60–120	215/210 <sup>c</sup>
<b>4c</b>		39, 63	87	119/120 <sup>c</sup>
<b>4d</b>	–24		105	128/132 <sup>c</sup>
<b>4e</b>				101

<sup>a</sup> sc = side chain. <sup>b</sup> lc = liquid crystalline. <sup>c</sup> Isotropization temperature from polarized optical microscopy.

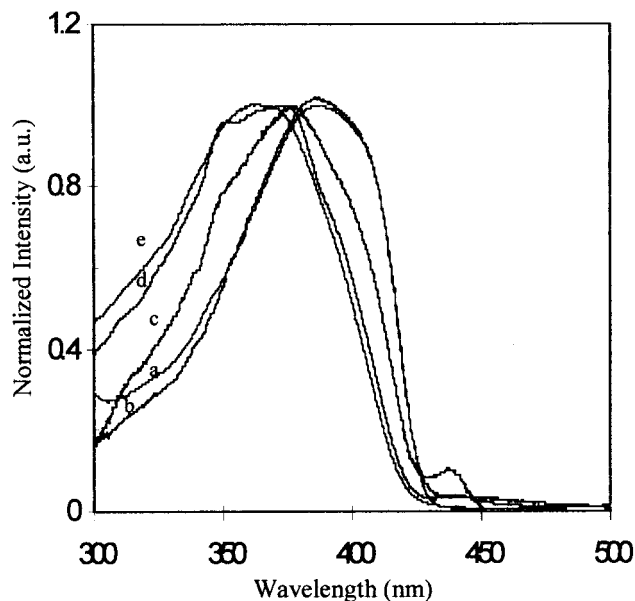


**Figure 7.** UV spectra of PPEs in toluene (0.0001 g/dL): (a) **4a**, (b) **4b**, (c) **4c**, (d) **4d**, and (e) **4e**.

to be 4.2 and 3.9 Å, indistinguishable from the stacking distances of the aromatic rings in PPE. For this reason we did not observe a separate set of X-ray reflections. The endotherm at 87 °C is again thought to represent a mesophase transition now that the side chains no longer hinder the translational motion of the rod. The last endotherm near 119 °C coincides with the isotropization temperature observed in POM and is caused by the disordering of the arrayed structure.

Among the five polymers studied, only the thermogram of **4d** (Figure 6d) shows a step change in specific heat below room temperature, which identifies itself as the glass transition temperature due to the motion of the branched 2-ethylhexyl groups. The shallow endotherm at 105 °C is again assigned as a mesophase transition followed by disordering/isotropization at 128 °C.

Interestingly, the thermogram of **4e** (Figure 6e) resembled that of **4a**, and only one transition was observed at 101 °C due to disordering. Although the distance between two aromatic planes is somewhat larger in **4e**, there is no noticeable difference in the disordering temperatures of **4a** and **4e**. The thermal transitions of each sample are summarized in Table 3.

**Photophysical Properties. UV Absorption Spectra.** The UV absorption spectra of PPE **4a–e** in toluene are shown in Figure 7, and the  $\lambda_{max}$  of all the PPEs are summarized in Table 4. The UV absorption spectra revealed that all five polymers have similar  $\pi-\pi^*$  transitions with  $\lambda_{max}$  at 388–368 nm (Table 4). The  $\pi-\pi^*$  transitions showed small and gradual blue shifts from **4a** to **4e**, suggesting decreasing electron delocal-



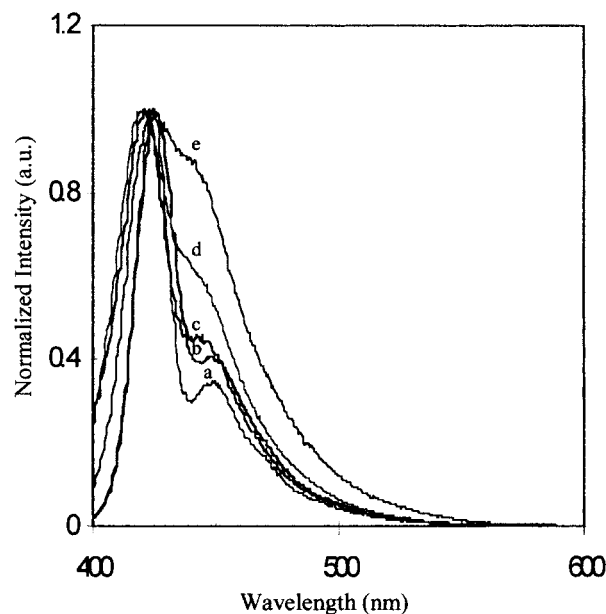
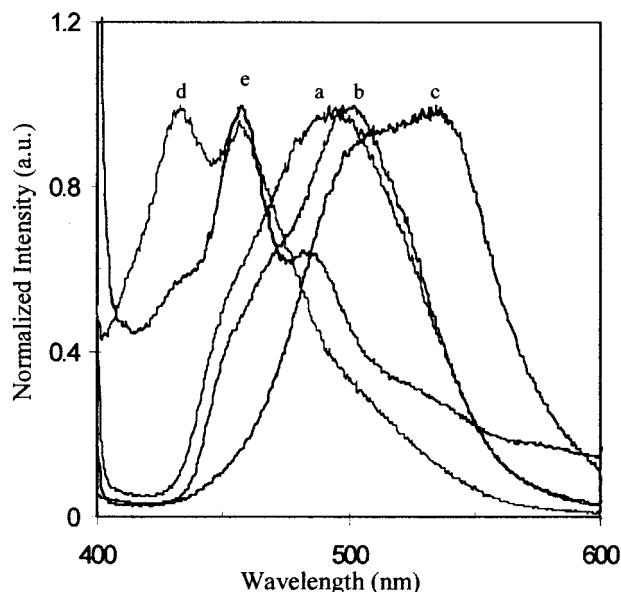
**Table 4. UV Absorption and Photoluminescence Properties of PPE 4a–e**

polymer	$\lambda_{\text{max}}$ (nm)			Stokes shift (nm)
	solution (UV)	solution (PL)	thin film (PL)	
<b>4a</b>	388	425 <sup>a</sup> /448 <sup>b</sup> (1/0.35) <sup>c</sup>	493 <sup>a</sup> /456 <sup>b</sup>	105 <sup>d</sup>
<b>4b</b>	384	426 <sup>a</sup> /448 <sup>b</sup> (1/0.41) <sup>c</sup>	502 <sup>a</sup> /463 <sup>b</sup>	108 <sup>d</sup>
<b>4c</b>	378	421 <sup>a</sup> /445 <sup>b</sup> (1/0.46) <sup>c</sup>	535 <sup>a</sup> /500 <sup>b</sup>	157 <sup>d</sup>
<b>4d</b>	374	422 <sup>a</sup> /444 <sup>b</sup> (1/0.60) <sup>c</sup>	433 <sup>a</sup> /455 <sup>b</sup>	59 <sup>d</sup>
<b>4e</b>	368	425 <sup>a</sup> /444 <sup>b</sup> (1/0.85) <sup>c</sup>	456 <sup>a</sup> /490 <sup>b</sup>	88 <sup>d</sup>

<sup>a</sup> Major peak. <sup>b</sup> Shoulder peak. <sup>c</sup> The ratio of major peak/shoulder peak intensities. <sup>d</sup> Calculated from major peaks.

ization along the chain as the side groups changed from dibutyl (PPE **4a**) to dioctyl (PPE **4b**), ditetradecyl (PPE **4c**), di-2-ethylhexyl (PPE **4d**), and di-2-cyclohexylethyl (PPE **4e**). The largest blue shift, 20 nm compared to PPE **4a**, was observed in PPE **4e** due to the bulkier side chains. Although the blue shift is only modest in magnitude, the introduction of various side groups on the phenyl rings indeed appears to affect the ground-state electronic structure of the PPEs as seen by comparing the absorption spectra of PPE **4e** (longer linear side chain), PPE **4d** (branched side chain), and PPE **4e** (bulky side chain) to that of PPE **4a**. However, the branched (PPE **4d**) or bulky (PPE **4e**) side groups caused larger changes in the electronic structure of the polymer than the linear side groups. These effects of branched and bulky substituents indicate that electron delocalization is reduced along the main chain since they impose a larger geometric effect on the ground-state electronic structure of the PPEs. Similar effects of intramolecular and supramolecular interactions on the photophysical properties of oligophenylene ethynyls have been found in single-crystal X-ray diffraction.<sup>10</sup> From studies of the oligophenylene ethynylene structures it is clear, for example, that the twist between adjacent planes of the phenyl rings of the main chain, which varies with the size of the side chain, causes lessened electron delocalization.

**Photoluminescence Spectra.** The photoluminescence spectra of the polymers were investigated in solution and in the solid state. The emission spectra in dilute toluene solutions (0.0001 g/dL) are shown in Figure 8, and the data are summarized in Table 4. PPE **4a–e** show very similar PL spectra in solution. The PL spectra are insensitive to the excitation wavelength in the range 330–400 nm. All the data given here were obtained by excitation at the wavelength of the respective absorption maximum. The splitting of the emission spectra into two well-resolved bands around 425 and 445 nm and the lack of mirror-image similarity between absorption and emission spectra can be attributed to vibronic coupling. The fact that the emission bands are much narrower than the absorption bands and show well-resolved vibronic bands is consistent with emission from localized excited states, most likely after a migration of the excitons along the polymer main chains to segments that represent low-energy states. Interestingly, we also found that the intensity of emission peak of lower energy state (ca. 445 nm) gradually increased as the side-group was changed from *n*-butyl to *n*-octyl, *n*-tetradecyl, 2-ethylhexyl, and 2-cyclohexylethyl. This indicates that the emission band at ca. 445 nm was strongly associated with the size and geometry of the side chain, which affected the torsion angle and the relative movement of the phenyl rings. Therefore, on the basis of similar findings by Friend et al.<sup>37</sup> in PPV

**Figure 8.** Fluorescence spectra of PPEs in toluene (0.001 g/dL): (a) **4a**, (b) **4b**, (c) **4c**, (d) **4d**, and (e) **4e**.**Figure 9.** Fluorescence spectra of pristine PPE films (spin-coated): (a) **4a**, (b) **4b**, (c) **4c**, (d) **4d**, and (e) **4e**.

studies, we tentatively conclude that the emission spectrum is characterized by a well-pronounced vibronic structure, which can be attributed to a coupling of the phenylene ring stretching modes of the main chain to the electronic transitions between  $\pi$  and  $\pi^*$  states.

The photoluminescence (PL) spectra of PPE **4a–e** thin films are shown in Figure 9, and the peak positions are listed in Table 4. By comparing the UV absorption spectra in solution with the PL spectra of the films, it can be seen that films of PPE **4a**, **4b**, and **4c** (linear side chains) have large Stokes shifts of 105–157 nm (Table 4), which is characteristic of excimer emission of solid films of many conjugated polymers.<sup>30</sup> On the other hand, PPE **4d** and **4e** have much smaller Stokes shifts (59 and 88 nm). Compared to PPE **4d** and **4e**, the polymers **4a**, **4b**, and **4c** have broad, featureless, emission bands that are also characteristic of excimers.<sup>30</sup> From the previous solid-state structure study and cited single-crystal X-ray diffraction structures of oligoPPEs,



it is known that the polymers with linear side-group substituents (PPE **4a**, **4b**, and **4c**) have essentially planar backbone structures with an intermolecular face-to-face distance of  $\sim 3.8$  Å. In contrast, the polymers with bulky side chains (PPE **4d** and **4e**) have noncoplanar structures and relatively large intermolecular distances of  $\sim 5.0$  Å. We therefore conclude that the solid-state emission of the PPE **4a–c** originates from excimers; however, the emission bands of PPE **4d** and **4e** are tentatively assigned to emission from intermolecular aggregates in view of their relatively large intermolecular distances.

## Conclusion

The following conclusions were reached. (1) X-ray diffraction studies indicated that the main chains of each polymer were arranged in regular, layered arrays where were characteristic of many rodlike polymers. (2) These layered arrays manifested themselves as liquid crystalline structures in PPEs **4b**, **4c**, and **4d**. (3) The temperatures of isotropization of the liquid crystalline structures in the three polymers coincided with the respective disordering temperatures determined by DSC. (4) With a long side chain C14, the endothermic transitions at 39 and 63 °C in the DSC thermogram were attributed to side chain melting, again a feature often observed in similar C14-substituted rigid polymers. (5) The UV absorption spectra of all five polymers revealed similar  $\pi-\pi^*$  transitions with  $\lambda_{\text{max}}$  at 388–368 nm. The gradual blue shift from **4a** to **4e** suggested decreasing electron delocalization along the chain as the side group changes from dibutyl to dioctyl, ditetradecyl, di-2-ethylhexyl, and di-2-cyclohexylethyl. These changes reflect the effects of side group length and geometry on the ground-state electronic structure of PPE. (6) The photoluminescence band for each polymer in dilute toluene solution shows two well-resolved bands, and the lack of mirror-image similarity between the absorption and emission spectra is indicative of vibronic coupling and is consistent with emission from localized excited states. (7) The photoluminescence spectra of thin films of **4a**, **4b**, and **4c**, when compared with their respective UV spectra, show large Stokes shifts, which are characteristic of excimers. Polymers with bulky substituents, **4d** and **4e**, showed smaller Stokes shifts, which could be rationalized by their noncoplanar structures and larger intermolecular distances. (8) The method developed in this study for the determination of molecular weight by end group analysis gave consistent results.

**Acknowledgment.** We thank the National Science Foundation, Division of Materials Research, under Grant DMR 9802108, for supporting this research.

## References and Notes

- Burroughes, J. H.; Bradley, D. D. C.; Brown, A. R.; Marks, R. N.; Mackay, K.; Friend, R. H.; Burns, P. L.; Holmes, A. B. *Nature* **1990**, *347*, 539.
- Montali, A.; Smith, P.; Weder, C. *Synth. Met.* **1998**, *Sept 15*, 123. (b) Neher, D. *Adv. Mater.* **1995**, *7*, 691.
- Kraft, A.; Grimsdale, A. C.; Holmes, A. B. *Angew. Chem.* **1998**, *37*, 403.
- Hide, F.; Diaz-Garcia, M. A.; Schwartz, B. J.; Heeger, A. J. *Acc. Chem. Res.* **1997**, *30*, 430.
- Pei, Q. B.; Yu, G.; Zhang, C.; Yang, Y.; Heeger, A. J. *Science* **1995**, *269*, 1086.
- Blom, P. W. M.; de Jong, M. J. M.; Vlegaar, *Appl. Phys. Lett.* **1996**, *68*, 3308.
- Weder, C.; Sarwa, C.; Montali, A.; Bastiaansen, C.; Smith, P. *Science* **1998**, *279*, 835.
- Heck, R. F. *Palladium Reagents in Organic Synthesis*; Academic Press: New York, 1990.
- Moroni, M.; Le Moigne, J.; Luzzati, S. *Macromolecules* **1994**, *27*, 562.
- Li, H.; Powell, D. R.; Hayashi, R. K.; West, R. *Macromolecules* **1998**, *31*, 52.
- Weder, C.; Wrighton, M. S. *Macromolecules* **1996**, *29*, 5175.
- Palmans, A. R. A.; Smith, P.; Weder, C. *Macromolecules* **1999**, *32*, 4677.
- Ziener, U.; Godt, A. *J. Org. Chem.* **1997**, *62*, 6137.
- Kloppenburger, L.; Jones, D.; Bunz, U. H. F. *Macromolecules* **1999**, *32*, 4194.
- Kloppenburger, L.; Jones, D.; Claridge, J. B.; zur Loye, H. C.; Bunz, U. H. F. *Macromolecules* **1999**, *32*, 4460. (b) Bunz, U. H. F.; Enkelmann, V.; Kloppenburger, L.; Jones, D.; Shimizu, K. D.; Claridge, J. B.; Zur Loye, H.-C.; Lieser, G. *Chem. Mater.* **1999**, *11*, 1416.
- Zhang, X.; Shetty, A. S.; Jenekhe, S. A. *Acta Polym.* **1998**, *49*, 52.
- Zhang, X.; Shetty, A. S.; Jenekhe, S. A. *Macromolecules* **1999**, *32*, 7422.
- Bao, Z.; Amundson, K. R.; Lovinger, A. J. *Macromolecules* **1998**, *31*, 8647.
- Tamao, K.; Sumitani, K.; Kiso, Y.; Zembayashi, M.; Fijioaka, A.; Kodama, S. I.; Nakajima, I.; Minato, A.; Kumada, M. *Bull. Chem. Soc. Jpn.* **1976**, *49*, 1958.
- Wang, P. W.; Lin, Y. J.; Devadoss, C.; Bharati, P.; Moore, J. S. *Adv. Mater.* **1996**, *8*, 237.
- Bao, Z.; Chan, W. K.; Yu, L. *J. Am. Chem. Soc.* **1995**, *117*, 12427.
- Yu, L. P.; Bao, Z.; Cai, R. B. *Angew. Chem., Int. Ed. Engl.* **1993**, *32*, 1345.
- Chen, S. H.; Mastrangelo, J. C.; Conger, B. M.; Kende, A. S.; Marshall, K. L. *Macromolecules* **1998**, *31*, 3391.
- Witteler, H.; Lieser, G.; Wenger, G.; Schulze, M. *Makromol. Chem., Rapid Commun.* **1993**, *14*, 471.
- Wautelet, P.; Moroni, M.; Oswald, L.; LeMoigne, J.; Pham, A.; Bigot, J. Y.; Luzatti, S. *Macromolecules* **1996**, *29*, 446.
- Gieser, R.; Schulz, R. C. *Makromol. Chem.* **1990**, *191*, 857.
- Cotts, P. M.; Swager, T. M.; Zhou, Q. *Macromolecules* **1996**, *29*, 7323.
- Bunz, U. H. F., et al. *Chem. Rev.* **2000**, *100*, 1605. (b) Gieser, R. J. *Macromol. Sci. Rev., Macromol. Chem. Phys.* **1996**, *C36*, 631.
- Steiger, D.; Smith, P.; Weder, C. *Macromol. Rapid Commun.* **1997**, *18*, 643.
- Halkyard, C. E.; Rampey, M. E.; Kloppenburger, L.; Studer-Martinez, S. L.; Bunz, U. H. F. *Macromolecules* **1998**, *31*, 8656. (b) Jenekhe, S. A.; Osaheni, J. A. *Science* **1994**, *265*, 765.
- Muller, A. *Proc. R. Soc. London, A* **1928**, *120*, 437.
- Broadhurst, M. G. *J. Res. Natl. Bur. Stand.* **1962**, *66A*, 241.
- Rodriguez-Parada, J. M.; Duran, R.; Wegner, G. *Macromolecules* **1989**, *22*, 2507.
- Lee, J. L.; Pearce, E. M.; Kwei, T. K. *Macromolecules* **1997**, *30*, 6877.
- Lee, J. L.; Pearce, E. M.; Kwei, T. K. *Macromol. Chem. Phys.* **1998**, *199*, 1003.
- Kaufman, H. S.; Sachse, A.; Alfreg, T. J.; Fankuchen, I. J. *Am. Chem. Soc.* **1948**, *76*, 6280.
- Friend, R. H.; Bradley, D. D. C.; Holmes, A. B. *Polym. LEDs. Phys. World* **1992**, *92*, 42.

MA001662B